Acta Crystallographica Section D
Biological Crystallography
ISSN 0907-4449

Expression and preliminary X-ray diffraction studies of cytosolic Cu,Zn superoxide dismutase from *Schistosoma mansoni*

Rosa M. F. Cardoso,[a,b] Carlos H. T. P. da Silva,[a] Ana P. U. de Araújo,[a] Tomoo Tanaka,[c,d] Manami Tanaka[c,e] and Richard C. Garratt[a]*

[a]Instituto de Física de São Carlos, Universidade de São Paulo, Av. Trabalhador Sancarlense 400, São Carlos, SP, 13566-590, Brazil, [b]Instituto de Química de São Carlos, Universidade de São Paulo, São Carlos, SP, 13566-590, Brazil, [c]The National Institute of Bioscience and Human Technology, Agency of Industrial Science and Technology, Tsukuba Science City, Ibaraki, 305-8566, Japan, [d]Tokai University School of Medicine, Isehara, Kanagawa 259-1193, Japan, and [e]The National Institute for Advanced Interdisciplinary Research, Agency of Industrial Science and Technology, Tsukuba Science City, Ibaraki 305-8562, Japan

Correspondence e-mail: richard@if.sc.usp.br

Received 27 April 2001
Accepted 6 September 2001

Active cytosolic (CT) Cu,Zn superoxide dismutase from *Schistosoma mansoni* (SmCTSOD) was recovered after thrombin cleavage of a glutathione-S-transferase linked fusion protein (GST-SmCTSOD) expressed in the presence of the active-site metals. Crystals have been obtained in two space groups, $P2_12_12_1$ and $P2_1$. The former have unit-cell parameters $a = 74.64$, $b = 78.24$, $c = 95.18$ Å and typically diffract to 2.2 Å. The monoclinic crystals have unit-cell parameters $a = 39.27$, $b = 95.08$, $c = 78.41$ Å, $\beta = 103.55^\circ$ and diffract to at least 1.55 Å. The calculated solvent content of the crystals is compatible with two dimers of SmCTSOD in the asymmetric unit in both cases. Molecular-replacement solutions have been obtained for both crystal forms and show that slight distortions in the crystal packing relate one form to the other.

1. Introduction

Cu,Zn superoxide dismutases (CuZnSODs) are metalloenzymes which protect cells from oxygen toxicity by catalysing the dismutation of the superoxide radical ($O_2^{\cdot-}$) into molecular oxygen and hydrogen peroxide (Fridovich, 1975). A widely accepted proposal for the catalytic mechanism of CuZnSODs involves the reduction of the oxidized Cu^{2+} form of the enzyme by superoxide, producing dioxygen, followed by the oxidation of the reduced Cu^{+} form by a second superoxide radical together with two protons, generating hydrogen peroxide.

Two forms of CuZnSODs have been identified in adult schistosomes, parasites responsible for the debilitating tropical disease known as bilhazia or schistosomiasis. The two forms are known as cytosolic SOD (SmCTSOD) (Simurda *et al.*, 1988; Hong *et al.*, 1992; Mei *et al.*, 1995) and signal peptide-containing SOD (SP-SOD, owing to the presence of a hydrophobic leader sequence). On infection by *S. mansoni*, the human host mounts an immune response that includes the production of free-radical oxidants by macrophages and leukocytes which enhances their capacity to kill schistosomes (Callahan *et al.*, 1988). One of the postulated mechanisms by which the parasites counterattack is the production of antioxidants (such as SODs) which act by destroying host-generated free radicals. These observations have led to the suggestion that *S. mansoni* SODs may represent a metabolic Achilles heel which might be exploited in the development of new therapeutic agents.

A homology-built model for SmCTSOD based on that from *Xenopus laevis* (Djinovic *et al.*, 1996) has revealed two substitutions relative to the human enzyme (E132L and K135V) within the entrance channel which leads to the active-site copper (Silva *et al.*, 2001). This observation has stimulated the current study of the crystallization of SmCTSOD with a view to determining its three-dimensional structure as an initial stage in the elaboration of specific inhibitors.

2. Methods and results

2.1. Protein expression and purification

Superoxide dismutase was expressed as a GST-SmCTSOD fusion protein in *Escherichia coli* BL21 (Novagen) with a prokaryotic expression vector containing an isopropyl-β-D-thiogalactoside (IPTG) inducible *tac* promoter. The bacteria were grown at 310 K in LB medium (1% bacto-tryptone, 0.5% yeast extract, 85 m*M* NaCl) with 100 µg ml^{-1} ampicillin for 12 h. The culture was then diluted 50-fold in prewarmed medium and grown to an optical density at 600 nm of approximately 0.6 before induction with 0.1 m*M* IPTG in the presence of 0.02 m*M* $CuCl_2$ and 0.02 m*M* $ZnCl_2$. These optimal values were established during pilot experiments in which the metal-ion concentration and time of addition were varied. Although large quantities of fusion protein are produced even in the absence of metal ions, the resulting enzyme proved to be catalytically inactive and presented a reduced secondary-structure content as monitored by

circular dichroism spectroscopy and FTIR, implying that the metal ions are important for correct folding (Lee *et al.*, 1996; Tanaka *et al.*, 1995). At concentrations of 1 m*M*, $CuCl_2$ and $ZnCl_2$ proved to be toxic to the cells and no recombinant protein was expressed.

After harvesting by centrifugation, cells were resuspended in 50 ml 0.15 *M* cold PBS buffer (140 m*M* NaCl, 2.7 m*M* KCl, 10 m*M* Na_2HPO_4, 1.8 m*M* KH_2PO_4) pH 7.4 containing 50 mg lysozyme. After an incubation step of 30 min on ice and subsequent sonication, the lysed cells were centrifuged at 17 000*g* for 20 min at 277 K. The supernatant was mixed with 2 ml of a 50% slurry of glutathione Sepharose 4B (Amersham Pharmacia Biotech.) preequilibrated with 0.15 *M* PBS. The suspension was incubated with gentle agitation for 3 h at 298 K and centrifuged at 500*g* for 5 min. The supernatant was removed and the resin pellet washed with 5 ml of PBS. After three washes with PBS, 2 ml of the buffer and 10 units of human thrombin (Novagen) were added. The mixture was incubated with gentle agitation for 15 h at 298 K and finally centrifuged under identical conditions. The supernatant was loaded onto a size-exclusion Superdex 75 column (Amersham Pharmacia Biotech.) equilibrated with 0.15 *M* PBS pH 7.4 and eluted in the same buffer. The resulting fractions were analyzed by 15% SDS–PAGE and those corresponding to SmCTSOD were of sufficient purity to yield diffraction-quality single crystals.

2.2. Crystallization

Crystallization trials were carried out by the hanging-drop vapour-diffusion method at 277 K using Crystal Screen kits I and II (Hampton Research) in drops composed of 5 µl of protein solution at a concentration of 4 mg ml^{-1} together with 5 µl of reservoir solution. After approximately two weeks, Crystal Screen I condition 10 (0.2 *M* ammonium acetate, 0.1 *M* sodium acetate buffer pH 4.6, 30% PEG 4000) produced single crystals of typical dimensions 0.1 × 0.1 × 0.1 mm (Fig. 1). Two different crystal forms, one orthorhombic and one monoclinic, grew under these conditions, as described below.

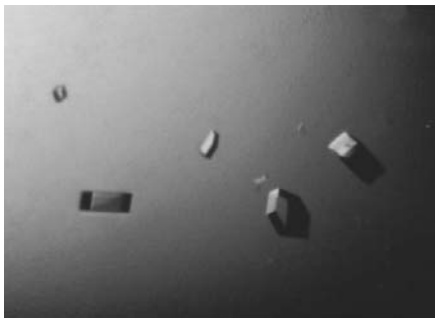

Figure 1
Crystals of SmCtTSOD of approximate dimensions 0.1 × 0.1 × 0.1 mm grown in 0.2 *M* ammonium acetate, 0.1 *M* sodium acetate buffer pH 4.6, 30% PEG 4000.

2.3. X-ray analyis

Data collection from the orthorhombic form to 2.2 Å resolution was performed with an R-AXIS II image-plate system mounted on a Rigaku RU-200 rotating-anode X-ray generator operating at 50 kV and 100 mA and using graphite monochromated Cu $K\alpha$ radiation (λ = 1.5408 Å). Data collection from the monoclinic form was performed at the protein crystallography beamline (Polikarpov *et al.*, 1998) of the Brazilian National Synchrotron Laboratory (LNLS), using a MAR345 image-plate detector and a wavelength of 1.54 Å. Diffraction data were collected and processed to only 1.55 Å owing to physical limitations, although it seems likely from the processing statistics that the crystals diffract to higher resolution.

All data were collected at 100 K with the crystals frozen in nylon loops in a solution containing 30% glycerol added to the mother liquor. 1° oscillation images covering a total angular ranges of 109 and 206° were collected using the R-AXIS II system and synchrotron radiation, respectively. The data were indexed and integrated with *DENZO* and merged with *SCALEPACK* from the *HKL* suite (Otwinowski & Minor, 1997).

2.3.1. Orthorhombic form. The SmCTSOD crystal (data collected using the R-AXIS II system) belongs to the space group $P2_12_12_1$ (as determined by systematic absences along all reciprocal axes), with unit-cell parameters a = 74.64, b = 78.24, c = 95.18 Å. The processing statistics of the final data set are given in Table 1. The calculated Matthews coefficient V_M of 2.22 Å^3 Da^{-1} suggests two SmCTSOD homodimers (MW = 15 682 Da per monomer) per asymmetric unit and a solvent content of 44.07% (Matthews, 1968).

The self-rotation function calculated with *GLRF* (Tong & Rossmann, 1990) showed no significant peaks besides those corresponding to crystallographic twofold axes in the section κ = 180°. On the other hand, a significant peak was observed in the native Patterson function at u = 0.50, v = 0.11, w = 0.00, calculated using all data from 100 to 2.2 Å with the program *CNS* (Brunger *et al.*, 1998), indicating the presence of non-crystallographic translational symmetry

Table 1
X-ray data-collection statistics.

Values in parentheses are for the highest resolution shell, which was 2.27–2.20 Å for the orthorhombic form and 1.59–1.55 Å for the monoclinic form.

	Orthorhombic	Monoclinic
X-ray source	Cu $K\alpha$	LNLS-CPr beamline
Wavelength (Å)	1.5408	1.5400
Total No. of reflections	171501	481989
No. of unique reflections	29152	81076
Space group	$P2_12_12_1$	$P2_1$
Unit-cell parameters (Å, °)	a = 74.64, b = 78.24, c = 95.18	a = 39.27, b = 95.08, c = 78.41, β = 103.55
Mosaicity (°)	0.28	0.25
Resolution (Å)	2.20	1.55
Completeness (%)	86.5 (72.9)	99.8 (98.9)
Reflections with $I > 3\sigma(I)$ (%)	81.3 (62.9)	91.2 (74.8)
R_{merge}†	0.080 (0.172)	0.051 (0.126)

† $R_{merge} = \sum I_i - \langle I \rangle / \sum I_i$, where I_i is an individual intensity observation, $\langle I \rangle$ is the mean intensity for that reflection and the summation is over all reflections.

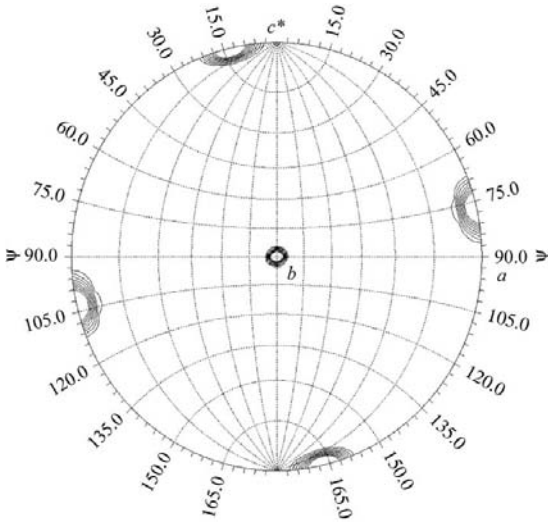

Figure 2
The self-rotation function (κ = 180°) for the monoclinic form, showing two related non-crystallographic peaks with correlation coefficients of 0.849. The contour levels are drawn at integral increments of the standard deviation (σ) beginning at 3.0σ.

relating the two dimers of the asymmetric unit (Fig. 2*a*). This was subsequently confirmed by molecular-replacement studies, as described below.

2.3.2. Monoclinic form. The SmCTSOD crystal collected using synchrotron radiation belonged to the space group $P2_1$, with unit-cell parameters a = 39.27, b = 95.08, c = 78.41 Å, β = 103.55°. These crystals grew under identical conditions to the orthorhombic form and were not obviously distinguishable visually. Table 1 gives the final processing statistics and the calculated Matthews coefficient of 2.26 Å^3 Da^{-1} once again corresponds to two dimers of SmCTSOD per asymmetric unit.

All significant peaks of the self-rotation function (calculated using reflections from 20.0 to 3.0 Å and an outer integration radius of 20.00 Å) were observed in the section corresponding to κ = 180°. Besides the crystallographic twofold axis along b, two further peaks with correlation coefficients of 0.849 were observed, corresponding to related non-crystallographic twofold axes at (φ, ψ) = (0, 78°) and (180, 12°) (Fig. 2*b*). In this case no significant peaks were observed in the native Patterson function, indicating the absence of non-crystallographic translational symmetry.

2.3.3. Molecular replacement. Initial phasing for both crystal forms was obtained by molecular replacement using the program *AMoRe* (Navaza, 1994) and the homology-built dimeric model of SmCTSOD as the search model. The latter was built using satisfaction of spatial restraints employing the program *MODELLER* (Sali & Blundell, 1993). It was based on the crystal structure of the Cu,Zn SOD from *X. laevis* which has been solved to 1.49 Å resolution and which presents 60% sequence identity with the *S. mansoni* enzyme. In the case of the orthorhombic crystals, employing data from 8.0 to 3.5 Å and an integration radius of 35.4 Å, a convincing solution was found for two dimers, yielding a correlation coefficient and R factor of 0.49 and 46.6%, respectively. For the monoclinic crystals, employing data within the same resolution range and an integration radius of 34.7 Å, the best solution for the two dimers gave a correlation coefficient of 0.72 and an R factor of 30.9%.

3. Discussion

As can be seen from Table 1, the b and c axes of the two crystal forms appear to be similar but have been exchanged during indexing. Furthermore, the a axis of the $P2_1$ crystals is very close to being half that of the $P2_12_12_1$ form, suggesting that the two lattices are closely related. The native Patterson function clearly shows that the non-crystallographic symmetry of the orthorhombic form corresponds principally to a translation of a/2. In the monoclinic form this non-crystallographic translation operator becomes a lattice translation along a; in this case, the non-crystallographic symmetry corresponds to a screw axis relating the two dimers of the asymmetric unit. This is a remnant of the crystallographic symmetry of the orthorhombic form and explains the strong non-crystallographic peaks in the self-rotation function, one of which lies approximately along the monoclinic a axis (Fig. 2*b*).

Fig. 3 shows the relationship between the two crystal forms in which alterations to the crystal packing lead to the interconversion between the crystallographic and the non-crystallographic symmetry described above. Packing forces are believed to be of particular relevance to the crystal structures of CuZnSODs, as it has been suggested that the redox state of the catalytic copper may be modulated by such effects. Hart *et al.* (1999) have analysed a wide variety of superoxide dismutases crystallized under different conditions and infer that the energy changes associated with crystal contacts may be sufficient to tip the balance between reduced and oxidized copper. In structural terms, this leads to alterations to the copper-ion coordination and in particular to the loss in the reduced form of the bridging histidine ligand (His63) which unites the two metal ions in the oxidized form. This analysis is complicated by the fact that different crystal forms of the same superoxide dismutase have generally been obtained under different conditions, meaning that crystal contacts are not the only variable under consideration. After full refinement, it will be of interest to evaluate the metal ion coordination of the two crystal forms reported here, as they have been grown under identical conditions and are expected to differ only in the crystal contacts made.

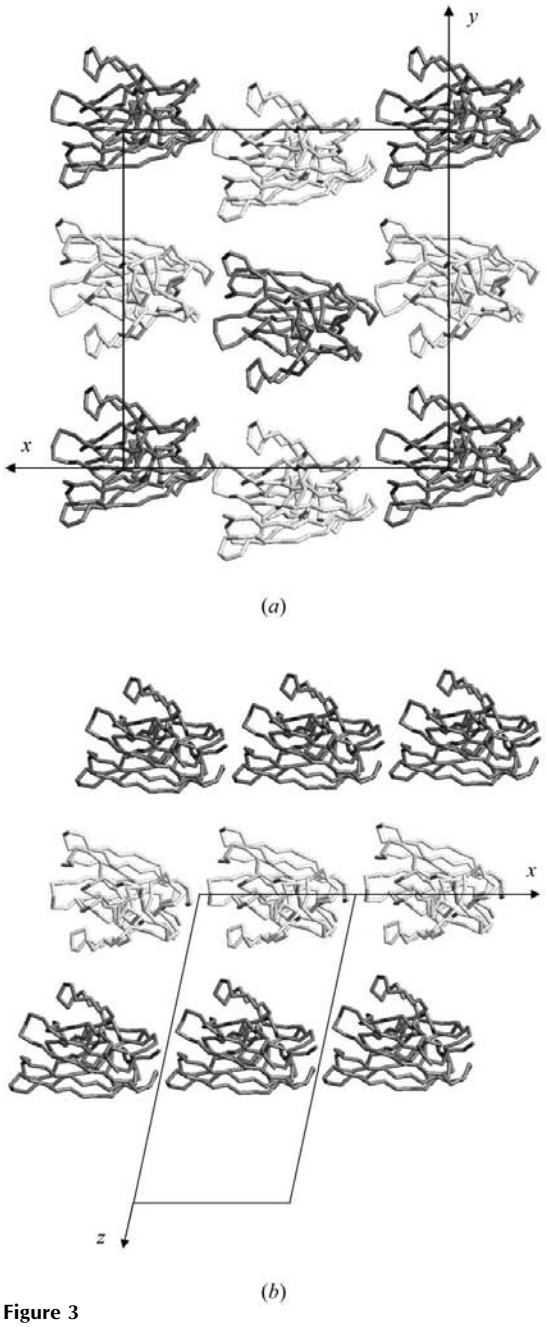

Figure 3
Molecular packing of the two crystal forms. A thin slice through the crystal parallel to the z axis, showing a single layer of molecules is shown in (*a*) for the orthorhombic form. In (*b*) the monoclinic form is viewed along the equivalent (y) direction. The crystallographically independent dimers are shaded differently and only a single subunit is shown in each case for reasons of clarity.

The refined structures will also be used in the improvement of novel SOD inhibitors currently under development. These are based on the presence of the hydrophobic residues Leu132 and Val135 which line part of the entrance channel leading to the active

site. This particular combination of hydrophobic residues has not yet been observed in previously reported crystal structures and may provide a route towards introducing specificity during inhibitor design.

We thank José Brandão Neto for excellent technical assistence in the use of the CPr beamline at the LNLS. This work was supported by grants from the Fundação de Amparo à Pesquisa do Estado de São Paulo (FAPESP) and PRONEX.

References

Brunger, A. T., Adams, P. D., Clore, G. M., DeLano, W. L., Gros, P., Grosse-Kunstleve, R. W., Jiang, J., Kuszewski, J., Nilges, M., Pannu, N. S., Read, R. J., Rice, L. M., Simonson, T. & Warren, G. L. (1998). *Acta Cryst.* D**54**, 905–921.

Callahan, H. L., Crouch, R. K. & James, E. R. (1988). *Parasitol. Today*, **4**, 218–225.

Djinovic, K., Battistoni, A., Carr, M. T., Polticelli, F., Desideri, A., Rotilio, G., Coda, A., Wilson, K. S. & Bolognesi, M. (1996). *Acta Cryst.* D**52**, 176–195.

Fridovich, I. (1975). *Annu. Rev. Biochem.* **44**, 147–159.

Hart, P. J., Balbirnie, M. M., Ogihara, N. L., Nersissian, A. M., Weiss, M. S., Valentine, J. S. & Eisenberg, D. (1999). *Biochemistry*, **38**, 2167–2178.

Hong, Z., LoVerde, P. T., Hammarskjold, M.-L. & Rekosh, D. (1992). *Exp. Parasitol.* **75**, 308–322.

Lee, J. K., Kim, J. M., Kim, S. W., Nam, D. H., Yong, C. S. & Huh, K. (1996). *Arch. Pharm. Res.* **19**, 178–182.

Matthews, B. W. (1968). *J. Mol. Biol.* **33**, 491–497.

Mei, H., Hirai, H., Tanaka, M., Hong, Z., Rekosh, D. & LoVerde, P. (1995). *Exp. Parasitol.* **80**, 250–259.

Navaza, J. (1994). *Acta Cryst.* A**50**, 157–163.

Otwinowski, Z. & Minor, W. (1997). *Methods Enzymol.* **276**, 307–326.

Polikarpov, I., Perles, L. A., de Oliveira, R. T., Oliva, G., Castelano, E. E., Garratt, R. & Craievich, A. (1998). *J. Synchrotron Rad.* **5**, 72–76.

Sali, A. & Blundell, T. L. (1993). *J. Mol. Biol.* **243**, 770–815.

Silva, C. H. T. P., Cardoso, R. M. F., Araujo, A. P. U., Tanaka, T., Tanaka, M. & Garratt, R. C. (2001). In preparation.

Simurda, M. C., Keulen, H. V., Rekosh, D. M. & LoVerde, P. T. (1988). *Exp. Parasitol.* **67**, 73–84.

Tanaka, K., Takio, S. & Satoh, T. (1995). *J. Plant. Physiol.* **146**, 361–365.

Tong, L. & Rossmann, M. G. (1990). *Acta Cryst.* A**46**, 783–792.